The Mechanism of Unimolecular Decomposition of CL-20 (2,4,6,8,10,12 Hexanitro-2,4,6,8,10,12-Hexaazaisowurtzitane). A Computational DFT Study

ARTICLE *in* THE JOURNAL OF PHYSICAL CHEMISTRY A · APRIL 2005

Impact Factor: 2.69 · DOI: 10.1021/jp045292v · Source: PubMed

5 AUTHORS, INCLUDING:

Sergiy I Okovytyy
Dnepropetrovsk National University
51 PUBLICATIONS **242** CITATIONS
SEE PROFILE

Yana Kholod
Monmouth University
25 PUBLICATIONS **233** CITATIONS
SEE PROFILE

The Mechanism of Unimolecular Decomposition of 2,4,6,8,10,12-Hexanitro-2,4,6,8,10,12-hexaazaisowurtzitane. A Computational DFT Study

Sergiy Okovytyy,[†,‡] Yana Kholod,[†,‡] Mohammad Qasim,[§] Herbert Fredrickson,[§] and Jerzy Leszczynski*[,‡]

Dnepropetrovsk National University, Dnepropetrovsk, 49050, Ukraine, Computational Center for Molecular Structure and Interactions, Jackson State University, Jackson, Mississippi, 39217, and US Army ERDC, Vicksburg, Mississippi 39180

Received: October 14, 2004; In Final Form: February 2, 2005

By using the B3LYP level of density functional theory, possible decomposition reaction pathways of 2,4,6,8,-10,12-hexanitro-2,4,6,8,10,12-hexaazaisowurtzitane (CL-20) in the gas phase have been investigated. We have found several types of reactions for this process: homolytic cleavage of an N−N bond to form the $NO_2^{\bullet}$ group; HONO elimination; C−C and C−N bonds breaking leading to ring opening; and H-migration. On the basis of the results of computation scanning of the potential energy surface, the most favorite pathway of CL-20 unimolecular decomposition that results in the formation of the stable aromatic compound 1,5-dihydrodiimidazo[4,5-*b*:4′,5′-*e*]pyrazine has been proposed.

Introduction

High-energy density materials play an important role in aeronautics, the weapons industry, and other high-tech fields in which cage structural compounds have generated popular interest due to their high density, high energy, and high tension. Since hexanitrohexaazaisowurtzitane (HNIW, CL-20, 2,4,6,8,-10,12-hexanitro-2,4,6,8,10,12-hexaazaisowurtzitane, 2,4,6,8,10,-12-hexanitro-2,4,6,8,10,12-hexaazatetracyclo[5.5.0.0.^{5,9}0^{3,11}]-dodecane) was first synthesized by Nielsen,[1] this family of compounds has become a focus in energetic research. This compound was recently proposed for military purposes and is expected to replace in many applications older and simpler analogues such as hexahydro-1,3,5-trinitro-1,3,5-triazine (RDX) and octahydro-1,3,5,7-tetranitro-1,3,5,7-tetrazocine (HMX).[2−4] These compounds are important energetic materials with applications ranging from explosives and rocket propellants to components of automobile air bags. They release large amounts of energy through a bulk decomposition process that is complex and involves both unimolecular and bimolecular reactions. An understanding of the complex chemical processes and an estimation of the influence of different factors on the reactivity of the titled explosives are essential for the design of efficient, environmentally benign applications for CL-20 utilization.

The toxicity and potential carcinogenicity of CL-20 and its transformation products has led to concerns about its fate in the environment and the potential for human exposure. Major transformation processes of this compound in the environment occur at moderate but variable rates leading to concerns about environmental risk.[5] In addition, many of the degradation products are more toxic than source compounds. Because of the highly exothermic nature of explosive materials, it is difficult to investigate many aspects of their reactivity with wet chemical

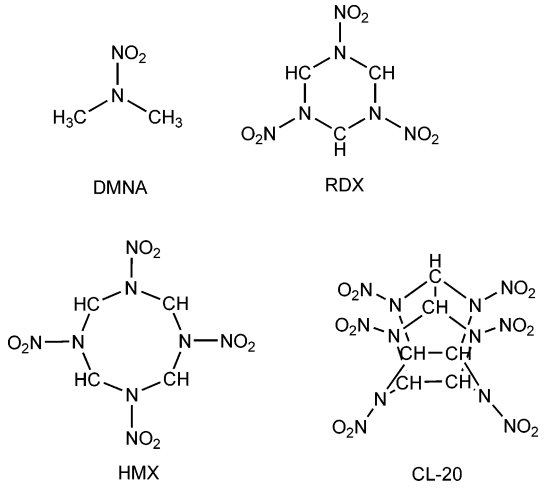

experimental techniques. However, quantum-chemistry methods offer risk-free and relatively accurate means to study their behavior.

A few experimental works including studies of synthesis pathways,[1,6] properties,[7−10] and different destruction methods[11−13] of CL-20 have been carried out. Stewart[14] and Dewar and Theil[15] calculated the geometric structures of CL-20 using the semi-empirical quantum chemical methods AM1 and PM3. Conformations of CL-20 have been investigated by Zhou et al. using the DFT level of theory.[16] Rice and Hare have predicted the heats of detonation of pure CL-20, using quantum-mechanical calculations.[17]

Different unimolecular degradation pathways for simpler cyclic nitramines, such as dimethylnitramine (DMNA),[18] RDX,[19−22] and HMX,[23−28] have been theoretically investigated. The following three types of reactions for cyclic nitramine decomposition have been defined:[23] (1) homolytic cleavage of an N−N bond accompanied by the elimination of the NO_2 group, (2) HONO elimination, and (3) ring-opening reactions.

The first process is the most favorable for the initial decompositions of nitramines to form corresponding radicals,

* Corresponding author. E-mail: jerzy@ccmsi.us.
† Dnepropetrovsk National University.
‡ Jackson State University.
§ US Army ERDC.

10.1021/jp045292v CCC: $30.25
Published on Web 03/08/2005

as it has been defined theoretically[18−20,23−27] and experimentally.[29−32] The N−N bond rupture is a reversible reaction.[27] In previous works[18−20,23,27] potential energy surface (PES) scanning of the $NO_2^•$ group homolytic elimination reaction has been performed for different nitramines. It has been shown that the N−N bond cleavage proceeds without a maximum, corresponding transition state, and a monotonic increase in energy with N−N distance stretching has been observed to approximately 3.8−3.9 Å. Further changing the N−N distance has not led to a significant increase in energy.

In the present work a quantum-chemical modeling of CL-20 unimolecular decomposition has been carried out.

Methodology

Johnson et al.[18] recently reported a detailed study of the performance of different nonlocal hybrid density functional theory (DFT) methods in comparison with the results of accurate quadratic configuration interactions with single and double excitations (QCISD) and with a correction for triple excitation (QCISD(T)) calculations for the $NO_2^•$ fission and HONO elimination from DMNA. They found that all considered DFT approaches (B1LYP, BHandHLYP, MPW1PW91, and B3LYP) perform well in predicting stationary-point geometries in comparison with those from the QCISD method. However, only the B1LYP and B3LYP methods with the Dunning's correlation consistent double-ξ plus polarization (cc-pVDZ) basis set could predict the reaction barriers for both the NO_2 and HONO elimination reactions to within 1 kcal/mol of those from the QCISD(T)//QCISD/cc-pVDZ calculations.

In the present work, geometry optimizations of all minima and transition state structures have been performed at the B3LYP/6-31G(d) level of theory.[33,34] Energies of all the considered systems have been computed by using the B3LYP/cc-pVTZ[33,35] level of theory.

The transition states have been verified to have only one imaginary frequency vibrational mode that connects the reactant and products. The $NO_2^•$ fission channel generates two free radicals; thus, the singlet open shell B3LYP method with a mix of the frontier molecular orbitals was adopted. Because this reaction channel has no barrier,[18−20,23,27] the reaction coordinate is approximated to correspond to the broken N−N bond distance, whereas other geometrical parameters are fully optimized. All electronic structure calculations were performed with the Gaussian 98 program.[36]

Results and Discussion

I. Conformations of CL-20. The basic structure of CL-20 (**1**) consists of a rigid isowurtzitane cage, which includes two five-member rings (FMRs) and a six-member ring (SMR). Two FMRs link each other by the C_1-C_7 bond at the top and project outward at two pairs of N atoms. There is considerable tension in the skeleton of CL-20. The C_1-C_7 bond linking the two FMRs and the six bonds of SMR are important stabilization factors. The SMR is boat-shaped with the prows directed downward.

The CL-20 molecule has six nitro groups attached to each of the six bridging nitrogen atoms in the cage (Figure 1). The spatial orientation of the nitro group has little influence on the skeleton. The N−N bonds of CL-20 are more fragile than the other bonds of **1**.

All spatial orientations of these nitro groups with respect to the FMRs and SMR in the cage, the differences in crystal lattice packing, and the number of molecules per unit cell define several possible polymorphs. So far, five polymorphs, a-, b-, g-, e-, and z-CL-20, have been isolated experimentally.[37−40] The relationships between the conformations and the molecular properties of CL-20 have been analyzed in detail by Zhou et al. in a previous work, using the B3LYP/6-31G(d,p) level of theory.[16] The authors have investigated the conformational properties of CL-20 and have shown that among four possible conformers (**1a**−**1d**), conformer **1d** (structure shown in Figure 2) is the most stable. In this study of decomposition mechanism, we have used the most stable conformation of CL-20 (**1d**).

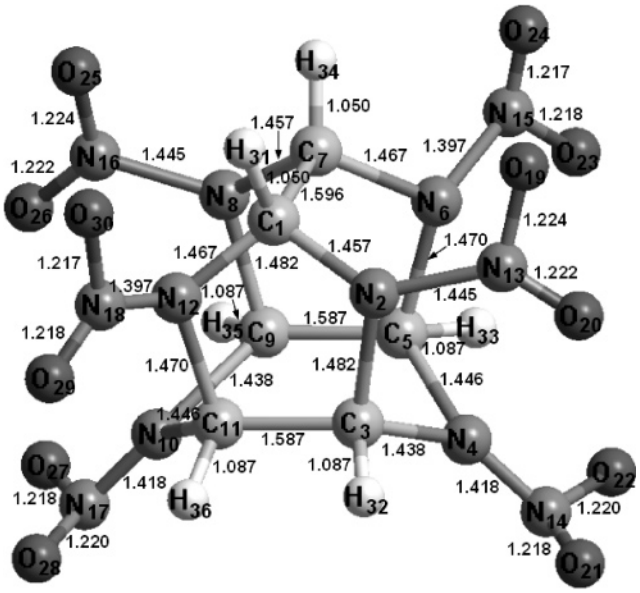

Figure 1. Optimized at the B3LYP/6-31G(d) level of the theory structure of CL-20.

II. Degradation Pathway. For the CL-20 unimolecular degradation process we have found several types of reactions: homolytic cleavage of an N−N bond accompanied by the elimination of $NO_2^•$ and a corresponding radical; HONO elimination to form a neutral nitramine; C−C and C−N bonds breaking leading to ring opening; and H-migration. Energies of all minima and transition states are given in Figure 3. The structures of the intermediates and products are shown in Figure 4. Figure 5 demonstrates geometric parameters of transition state structures.

Initiation of Decomposition. Since the molecular structure of CL-20 is characterized by $NO_2^•$ groups of two different types (four groups in FMRs and two in the SMR), it is likely that there will be preferential elimination of one type of $NO_2^•$ group over the other. There are also two possible types of HONO elimination reactions. We have explored all these possibilities.

At the first step the energies of both N_2-N_{13} (analogue N_6-N_{15}, N_8-N_{16}, $N_{12}-N_{18}$) and N_4-N_{14} (analogue $N_{10}-N_{17}$) bond rupture processes that are accompanied by the elimination of $NO_2^•$ or HONO species have been computed.

Figure 3 clearly shows that removal of the $NO_2^•$ radical from a FMR location generates the most stable radical INT11 with a reaction energy of 37.6 kcal/mol, whereas an energy value of 41.1 kcal/mol is required to remove one $NO_2^•$ group from the SMR. There are no critical points on the PES of the N−N bond cleavage to form the NO_2 radical. We have scanned the PES of the $NO_2^•$ radical elimination to form INT11 and INT12 and found a monotonic increase in energy proportionate to an increase in the N−N bond length. After the bond length approaches 3.8−3.9 Å, the energy of such a conformation is approximately equal to the energy of the N−N bond fission reaction.

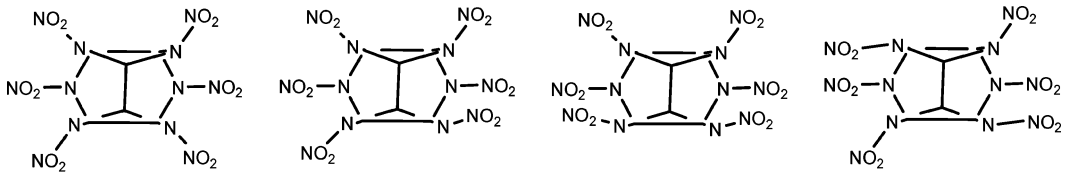

1a 1b 1c 1d

Figure 2. The conformations of CL-20.

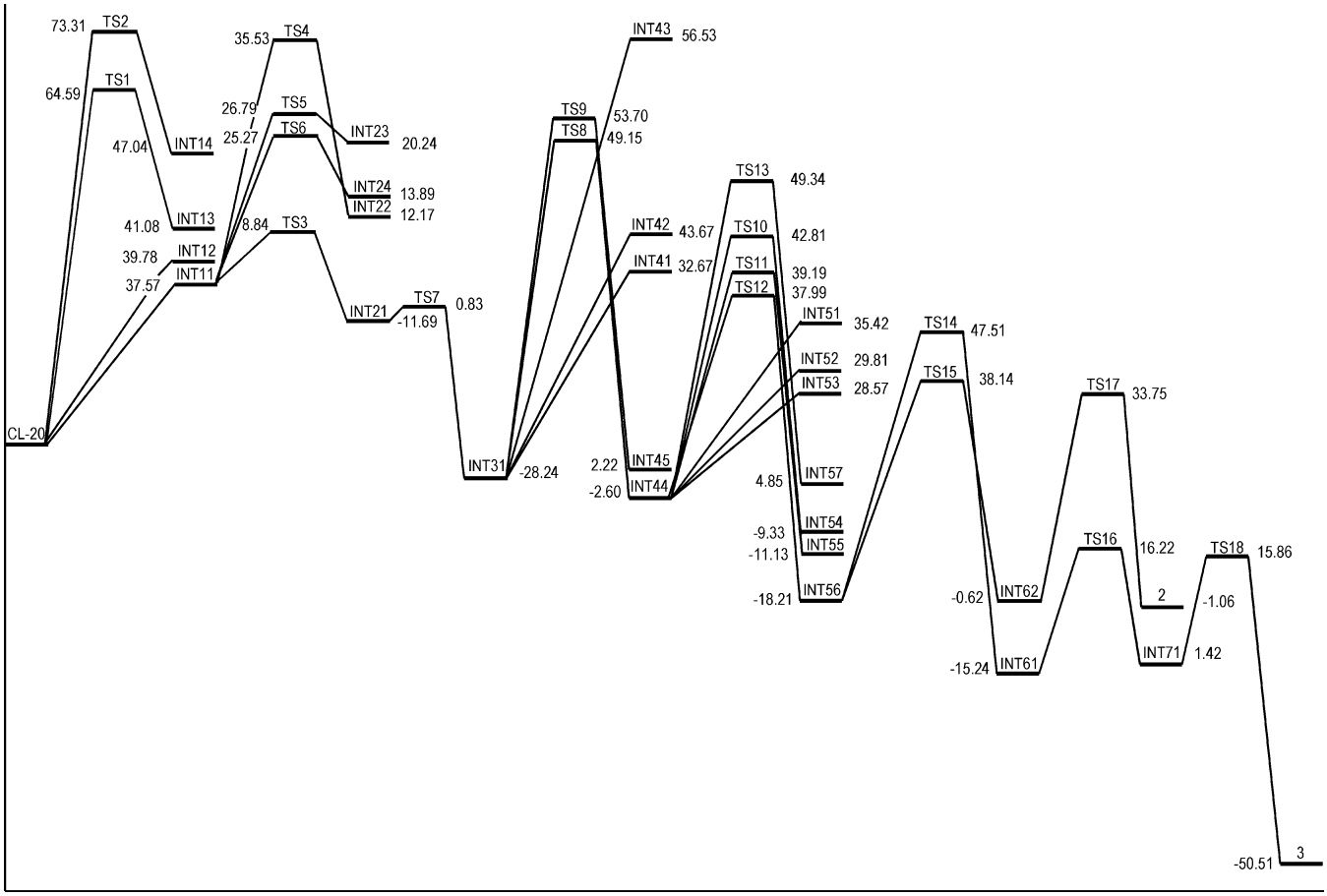

Figure 3. Potential energy profile for CL-20 unimolecular degradation; energies are in kcal/mol.

The concerted HONO elimination involves breaking both the N−N and C−H bonds. The short nonbonded N−O···H−C distance plays an important role in the HONO elimination. This distance is smaller for NO_2 groups, connected to the FMR.

Because of NO_2 located at the five-membered-ring bond and the closer nonbonded O···H distance, the concerted HONO elimination will preferentially occur to form INT13 and INT14 (39.8 and 41.7 kcal/mol, respectively).

The activation barriers for reactions passing through TS1 and TS2 of the aforementioned HONO elimination reactions are equal to 64.6 and 73.3 kcal/mol, respectively.

On the basis of these results, we have chosen the homolytic $NO_2^{\bullet}$ elimination from the FMR to form INT11 as the most favorable process for the initial stage of CL-20 unimolecular decomposition.

INT11 Ring-Opening Reactions. At the second stage there are four possible ways to open the ring of formed polycyclic radical INT11: (1) C_1-C_7 bond, connecting two FMRs, rupture to form INT21, (2) C_1-N_2 bond of FMR, cleavage to form INT22, (3) C_3-C_{11} bond of SMR, rupture to form INT23, and (4) $N_{10}-C_{11}$ bond of SMR, cleavage to form INT24.

Simultaneously a neighboring C−N bond gains double character.

The first pathway according to calculations characterizes the lowest energy decomposition of INT11. The ring-opened structure INT21 is 11.7 kcal/mol more stable than INT11. The ring opening of INT11 occurs through the breaking of the C_1-C_7 bond between two FMRs. The $C_1\cdots C_7$ bond in TS3 breaks at a distance of 2.059 Å. The activation barrier of this process is equal to 8.8 kcal/mol. INT21 is the ring-open structure of INT11 as shown in Figure 4. In TS3 the $H_{31}C_1-N_{12}$ group of FMR has a $C_1=N_{12}$ double bond length of 1.336 Å (compared to the similar C_1-N_{12} bond in INT11, 1.467 Å). The distance of the $C_1\cdots C_7$ bond in INT21 is 3.522 Å.

The corresponding TS4, TS5, and TS6 transition state species have been located on the PES of the second, third, and forth reactions. It has been found that the ring-opened structures INT22, INT23, and INT24 are 12.2, 20.2, and 13.9 kcal/mol, respectively, less stable than INT11. These processes have significantly higher activation energies compared to reaction 1 (26.7, 17.9, and 16.4 kcal/mol, respectively).

Decomposition of the INT21 Radical. Clearly, the ring-opened INT21 radical is stabilized by the N_6-N_{15} bond homolytic fission to form a neutral molecule INT31 with a low energetic barrier (0.8 kcal/mol). The energy of reaction is equal to −28.2 kcal/mol. Simultaneously, the $N_6=C_7$ bond gains double

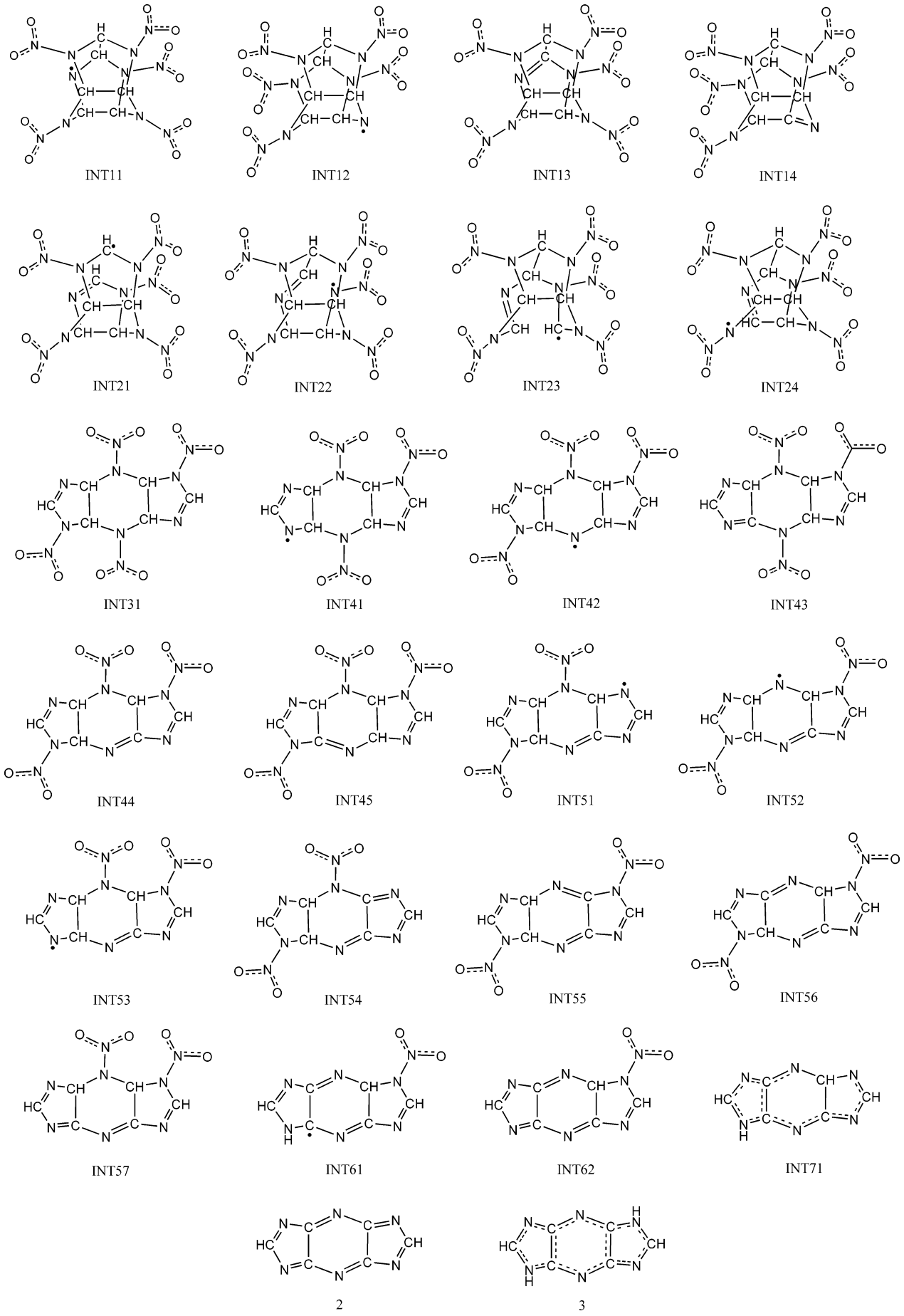

Figure 4. Intermediates and products of CL-20 unimolecular degradation.

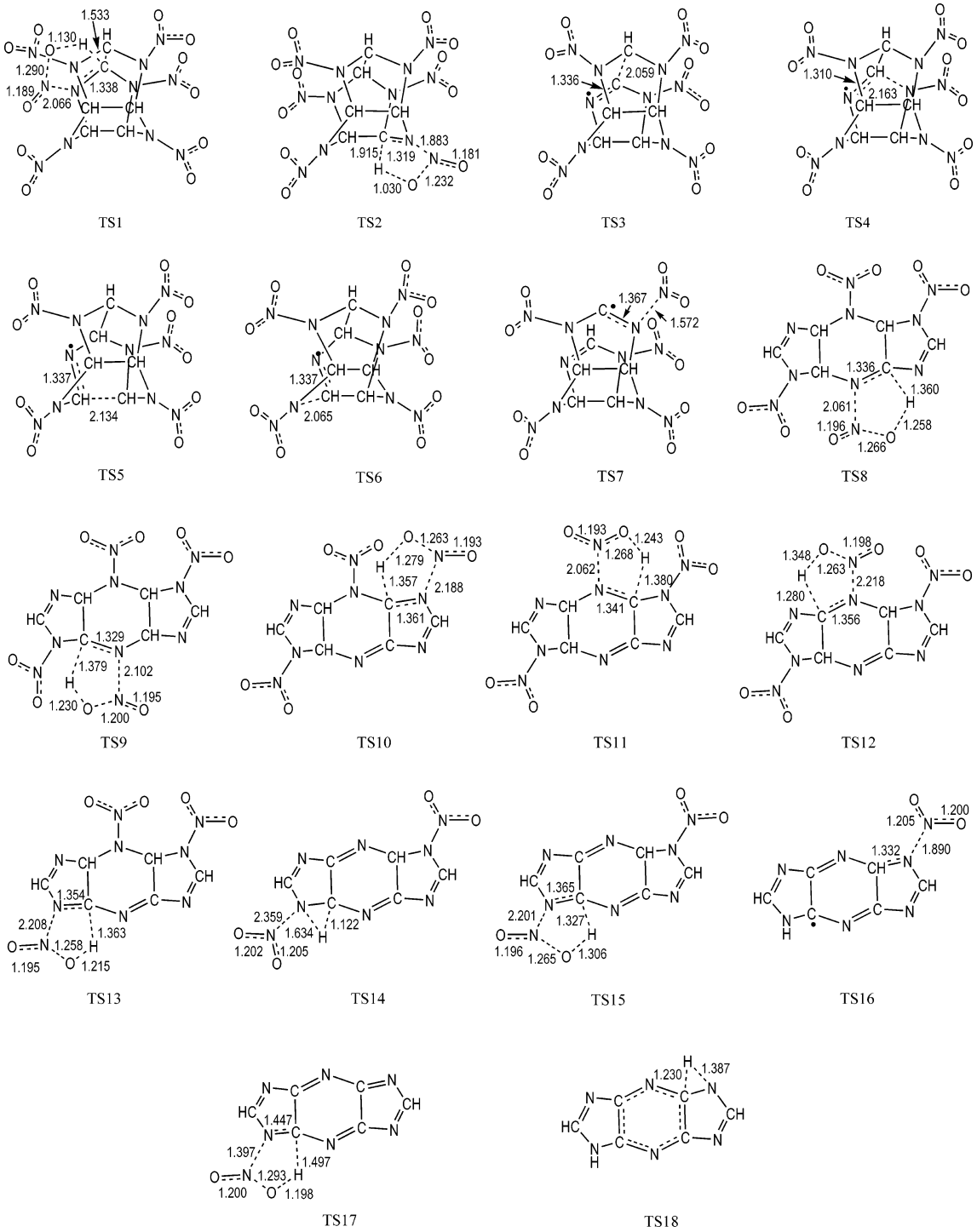

Figure 5. Geometric parameters of transition states structures of CL-20 unimolecular degradation.

character. The N···N bond length of the corresponding TS7 is equal to 1.572 Å, and N_6═C_7 becomes 0.09 Å shorter, compared with INT21.

Decomposition of INT31. We have explored five possible pathways of INT31 degradation to form INT41, INT42, INT43, INT44, and INT45, as shown in Figure 4.

The elimination of the next $NO_2^•$ group from INT31 involving N_2-N_{13} or N_4-N_{14} homolytic cleavage requires an additional 32.7 and 43.7 kcal/mol to form INT41 and INT42, respectively. The formation of these radical intermediates does not have any appreciable reaction barrier similar to the formation of INT11 from CL-20.

Instead of the elimination of the $NO_2^•$ group, an alternate pathway for the decomposition of INT31 might include HONO elimination and subsequent decomposition. On the basis of the close nonbonded contact of the H atom and the NO_2 group in analogous cyclic nitramine RDX, the possibility for H-migration or HONO elimination from RDX was suggested by Harris and Lammertsma.[39]

In the first case HONO elimination takes place via the elimination of the $NO_2^•$ group of FMR and the neighboring C_3H_{32} group hydrogen of SMR to form INT43. This process is highly endothermic (56.5 kcal/mol), so one can assume that the activation barrier of the reaction is just as high, and this is the least probable process.

Two other possible pathways of HONO elimination differ by a double C═N bond position in a formed intermediate. The INT44 generating reaction is 4.8 kcal/mol more exothermic

compared to the INT45 formation, due to the two double N_4═C_5 and N_6═C_7 bond conjugations which occur in the case of INT44.

The length of the broken N_4···N_{14} bond in TS8 is 2.061 Å, and the transferred H_{33} atom is 1.360 and 1.258 Å away from the C_5 and O_{22} atoms, respectively. The formation of the N_4═C_5 bond results in more planar character of INT43. The reaction through TS8 is characterized by a barrier of 49.1 kcal/mol.

In TS9 the breaking N_4···N_{14} distance is equal to 2.102 Å. The transferring H atom is 1.379 and 1.230 Å away from the C_3 and O_{21} atoms, respectively. The activation barrier of the reaction through TS9 is equal to 53.7 kcal/mol.

Despite the high activation energy for INT44 and the lower energies necessary for the formation of INT41 and INT42, we suppose that, taking into account the reversible character of the $NO_2^•$-elimination reactions,[27] the generation of the most stable thermodynamically controlled INT44 is a preferable process.

Decomposition of INT44. INT44, having three $NO_2^•$ groups, as shown in Figure 4, can be decomposed in seven different ways to form three products of NO_2-radical elimination and four of HONO elimination.

At the first step of the INT44 decomposition, the investigations of the elimination of three $NO_2^•$ groups to form INT51, INT52, and INT53 have been performed. The formation processes of INT51 and INT52 require additional energy of 28.6 and, 29.8 kcal/mol, while the INT53 generation reaction is highly endothermic (35.4 kcal/mol).

We have examined four possible pathways of HONO elimination from INT44 and found that there are two N−N fissions at FMR (N_2−N_{13} and N_8−N_{15}), when the nearest hydrogen atom of SMR is transferred from the carbon to the oxygen atom. There are more endothermic reactions which have higher activation barriers compared to cases where SMR is a donor of the $NO_2^•$ group. Thus, the reaction channels through TS10 and TS13 leading to INT54 and INT57 have barriers of 42.8 and 49.3 kcal/mol, respectively. The activation barriers of the INT55 and INT56 formation reactions, characterized by TS11 and TS12, are close in energy (39.2 and 38.0 kcal/mol), but the second process is 9.1 kcal/mol more exothermic, because of the formation of compound, containing two conjugated couples of double N═C bonds (N_4═C_5 and N_6═C_7; N_{10}═C_{11} and N_{12}═C_1).

The broken N···N bonds in TS10, TS11, TS12, and TS13 are characterized by bond distances 2.188, 2.062, 2.218, and 2.208 Å, and the broken C···H bond lengths are equal to 1.357, 1.380, 1.280, and 1.363 Å. On the other hand, the formed O···H bonds are characterized by bond distances of 1.279, 1.243, 1.348, and 1.215 Å, and the formed C···N π-bonds are equal to 1.361, 1.341, 1.356, and 1.354 Å, respectively. Due to the formation of a C−N π-bond via the elimination of HONO in INT55 and INT56, the neighboring $NO_2^•$ group rearranges from an axial to an equatorial orientation, which is accompanied by the flattening of the tricyclic structure. INT56 has a longer C−N double bond of 1.337 Å compared to INT54 (1.272 Å), INT55 (1.289 Å), and INT57 (1.277 Å), due to the significant delocalization of the π electrons in the formed triene system in INT56.

Decomposition of INT56. We have found two possible pathways of further INT56 decomposition.

(*a*) *Consecutive Elimination of HONO.* HONO elimination from INT56 has a small exothermic effect (0.6 kcal/mol), due to the formation of three conjugated C═N double bonds (INT62). The N_2···N_{13} distance is equal to 2.201 Å, the broken C_3···H_{32} bond length is 1.327 Å, whereas the formed O_{20}···H_{32} bond is 1.306 Å, and the formed C_3···N_2 π-bond distance is equal to 1.365 Å in the corresponding TS15.

The last removal of the $NO_2^•$ group through HONO elimination from INT62 to form compound **2** is slightly exothermic, analogous to the transformation of INT56 to INT62. The product **2** is 1.1 kcal/mol more stable than INT62. The activation barrier of this process is equal to 33.8 kcal/mol, and the geometric parameters of the corresponding broken and formed bonds of TS17 are similar to those of TS15.

(b) Consecutive Elimination of Two $NO_2^•$ Groups, Accompanied by the H Atom Migration from the C Atom to the N Atom. The homolytic N_2···N_{13} bond rupture of INT56 becomes difficult due to the formation of a radical. This transformation can be facilitated by the H_{32} atom migration with simultaneous $NO_2^•$ elimination. This leads to TS14, as shown in Figure 5. As the N_2···N_{13} bond distance increases in TS14, the H_{32} atom migrates from the C_3 to the N_2 atom. The length of the broken N_2···N_{13} bond in TS14 is 2.359 Å, and the migrating H_{32} atom is 1.634 and 1.122 Å away from the N_2 and C_3 atoms, respectively. The reaction has a barrier of 47.5 kcal/mol over INT56 and yields INT61. This one is a relatively stable intermediate with 15.2 kcal/mol of exothermic energy compared to INT56.

We have investigated the possible pathway of the last $NO_2^•$ group elimination facilitated by the simultaneous H_{35} atom migration from INT61. In contrast to the $NO_2^•$ group elimination from neutral molecule INT56 with the generation of two radicals, the removal of the $NO_2^•$ group from the INT61 radical to form neutral INT71 does not lead to simultaneous H-migration. Formed INT71 is 1.4 kcal/mol less stable compared to INT61. The reaction proceeds through TS16 with a 16.2 kcal/mol barrier. The length of the breaking N_8···N_{16} bond in TS17 is equal to 1.890 Å, and the formed C···N π-bond is 1.332 Å.

Following H_{35} migration from the C_9 to the N_8 atom to form aromatic compound 1,5-dihydrodiimidazo[4,5-*b*:4′,5′-*e*]pyrazine (**3**) is achieved in the next step. TS18 has been located at the PES of this reaction, which requires an additional 15.9 kcal/mol of energy. The migrating H_{35} atom is 1.387 and 1.230 Å away from the N_8 and C_9 atoms in TS18. The obtained aromatic product (**3**) is 50.5 kcal/mol more stable than INT71. The formation of an aromatic structure (**3**) has been confirmed by UV/VIS and FTIR spectra for other CL-20 decomposition processes: alkaline hydrolyses, reported by Qasim and et al.[42]

Conclusion

We have studied several types of reactions for the CL-20 unimolecular degradation process: homolytic cleavage of an N−N bond accompanied by the elimination of $NO_2^•$ and a corresponding species, HONO elimination, and C−C and C−N bond breakage leading to the ring opening.

At the first step of the study, the energies of both of the FMR and SMR N−N bonds rupture processes that are accompanied by the elimination of the $NO_2^•$ or HONO species have been computed. It has been concluded that the homolytic $NO_2^•$ group elimination from FMR is the least endothermic. The C_1−C_7, C_5−C_9, N_4−C_5, and C_7−N_8 bond cleavages of INT11 have been modeled. The minimum energy corresponds to the C_1−C_7 bond breaking reaction. Simultaneously, the C_1−N_{12} bond gains double character. The elimination of the $NO_2^•$ group from the N_6 atom and the N_6═C_7 double bond formation leads to significant stabilization of the system due to the transformation of the radical INT21 to the neutral species INT31. The most favorable pathway of INT31 decomposition is HONO elimination with the formation of a neutral INT44 molecule with two

conjugated double bonds $C_4{=}N_5$ and $N_6{=}C_7$. The breaking of the $N_{10}{-}N_{17}$ and $C_{11}{-}H_{36}$ bonds with HONO and formation of the neutral molecule INT56, containing two couples of conjugated double bonds, is the most advantageous of all possible ways of INT44 destruction through $NO_2^{\bullet}$ or HONO elimination. During the next steps two successive $NO_2^{\bullet}$ radical eliminations follow and yield molecules (INT61 and INT71) which are stabilized by the migration of hydrogen from the C_3 and C_9 atoms to the N_2 and N_8 atoms, accordingly.

CL-20 unimolecular decomposition results in the formation of the aromatic compound 1,5-dihydrodiimidazo[4,5-*b*:4′,5′-*e*]-pyrazine (**3**).

Acknowledgment. This work was facilitated by ERDEC grant No. W912HZ-04-P-0139, a NATO grant No. PST.NUKR.CLG 981073, and the support of the Army High Performance Computing Research Center under the auspices of the Department of the Army, Army Research Laboratory cooperative agreement No. DAAD19-01-02-0014, and the Army Corps of Engineers Environmental Quality and Installations Research and Development Program. The content of this paper does not necessarily reflect the position or policy of the government, and no official endorsement should be inferred.

References and Notes

(1) Nielsen, A. T.; Chafin, A. P.; Christian, S. L.; Moore, D. W.; Nadler, M. P.; Nissan, R. A.; Vanderah, D. J.; Gilardi, R. D.; George, C. F.; Flippen-Anderson, J. L. *Tetrahedron* **1998**, *54*, 11793.

(2) Andrews, D. H. *Phys. Rev.* **1990**, 36, 544

(3) Holtz, E. V.; Ornellas, D. O.; Foltz, M. F. *Propellants, Explos., Pyrotech.* **1994**, *19*, 206.

(4) Foltz, M. F. *Propellants, Explos., Pyrotech.* **1994**, *19*, 63.

(5) Szecsody, J. E.; Girvin, D. C.; Devary, B. J.; Campbell, J. A. *Chemosphere* **2004**, *56*, 593.

(6) Clawson, J. S.; Anderson, K. L.; Pugmire, R. J.; Grant, D. M. *J. Phys. Chem. A* **2004**, *108*, 2638.

(7) Monteil-Rivera, F.; Paquet, L.; Deschamps, S.; Balakrishnan, V. K.; Beaulieu, C.; Hawari, J. *J. Chromatogr. A* **2004**, *1025*, 125.

(8) Sorescu, D. C.; Rice B. M.; Thompson, D. L. *J. Phys. Chem. B* **1998**, *102*, 948.

(9) Sikder, A. K.; Maddala, G.; Agrawal, J. P.; Singh, H. *J. Hazard. Mater.* **2001**, *A84*, 1.

(10) Sorescu, D. C.; Rice, B. M.; Thompson, D. L. *J. Phys. Chem. B* **1999**, *103*, 6783.

(11) Bellamy, A. J. *Tetrahedron* **1995**, *51*, 4711.

(12) Bohn, M. A. *Thermochim. Acta* **2003**, *401*, 27.

(13) Yang, R.; An, H.; Tan, H. *Combust. Flame* **2003**, *135*, 463.

(14) Stewart, J. J. P. *J. Comput. Chem.* **1989**, *10*, 209.

(15) Dewar, M. S. J.; Theil, W. *J. Am. Chem. Soc.* **1997**, *99*, 44899.

(16) Zhou, G.; Wang, J.; He, W.-D.; Wong, N.-B.; Tian, A.; Li, W.-K. *J. Mol. Struct.* (*THEOCHEM*) **2002**, *589*−*590*, 273.

(17) Rice, B. M.; Hare, J. *Thermochim. Acta* **2002**, *384*, 377.

(18) Johnson, M. A.; Truong, T. N. *J. Phys. Chem. A* **1999**, *103*, 8840.

(19) Wu, C. J.; Fried, L. E. *J. Phys. Chem. A* **1997**, *101*, 8675.

(20) Chakraborty, D.; Muller, R. P.; Dasgupta, S.; Goddard, W. A., III. *J. Phys. Chem. A* **2000**, *104*, 2261.

(21) Just, C.; Schnoor, J. *Environ. Sci. Technol*. **2004**, *38*, 290.

(22) Long, G. T.; Vyazovkin, S.; Brems, B. A.; Wight, C. A. *J. Phys. Chem. B* **2000**, *104*, 2570.

(23) Chakraborty, D.; Muller, R. P.; Dasgupta, S.; Goddard, W. A., III. *J. Phys. Chem. A* **2001**, *105*, 1302.

(24) Zhang, S.; Truong, T. N. *J. Phys. Chem. A* **2000**, *104*, 7304.

(25) Zhang, S.; Truong T. N. *J. Phys. Chem. A* **2001**, *105*, 2427.

(26) Zhang, S.; Nguyen, H. N.; Truong, T. N. *J. Phys. Chem. A* **2003**, *107*, 2981.

(27) Lewis, J. P.; Glaesemann, K. R.; VanOpdorp, K.; Voth, G. A. *J. Phys. Chem. A* **2000**, *104*, 11384.

(28) Manaa, M. R.; Fried, L. E.; Melius, C. F.; Elstner, M.; Frauenheim, Th. *J. Phys. Chem. A* **2002**, *106*, 9024.

(29) Belyayeva, M. S.; Klimenko, G. K.; Babaytseva, L. T.; Stolyarov, P. N. *5th All Union Symp. Combust. Deton.* **1977**, 53.

(30) McMillen, D. F.; Barker, J. R.; Lewis, K. E.; Trevor, P. L.; Golden, D. M. SRI Project PYU-5787, 1979.

(31) Maksimov, Y. Y.; Apol'kova, V. N.; Braverman, O. V.; Solov'en, A. I. *Russ. J. Phys. Chem.* **1985**, *59*, 9.

(32) Burov, Y. M.; Nazin, G. M. *Kinet. Catal.* **1982**, *23*, 5.

(33) Becke, A. D. *J. Chem. Phys.* **1993**, *98*, 5648.

(34) Ditchfield, R.; Hehre, W. J.; Pople, J. A. *J. Chem. Phys.* **1971**, *54*, 724.

(35) Kendall, R. A.; Dunning, T. H., Jr.; Harrison R. J. *J. Chem. Phys.* **1992**, *96*, 6796.

(36) Frisch, M. J.; Trucks, G. W.; Schlegel, H. B.; Scuseria, G. E.; Robb, M. A.; Cheeseman, J. R.; Zakrzewski, V. G.; Montgomery, J. A., Jr.; Stratman, R. E.; Burant, J. C.; Dapprich, S.; Millam, J. M.; Daniels, A. D.; Kudin, K. N.; Strain, M. C.; Farkas, O.; Tomasi, J.; Barone, V.; Cossi, M.; Cammi, R.; Mennucci, B.; Pomelli, C.; Adamo, C.; Clifford, S.; Ochterski, J.; Petersson, G. A.; Ayala, P. Y.; Cui, Q.; Morokuma, K.; Salvador, P.; Dannenberg, J. J.; Malick, D. K.; Rabuck, A. D.; Raghavachari, K.; Foresman, J. B.; Cioslowski, J.; Ortiz, J. V.; Baboul, A. G.; Stefanov, B. B.; Liu, G.; Liashenko, A.; Piskorz, P.; Komaromi, I.; Gomperts, R.; Martin, R. L.; Fox, D. J.; Keith, T.; Al-Laham, M. A.; Peng, C. Y.; Nanayakkara, A.; Challacombe, M.; Gill, P. M. W.; Johnson, B.; Chen, W.; Wong, M. W.; Andres, J. L.; Gonzalez, C.; Head-Gordon, M.; Replogle, E. S.; Pople, J. A. *Gaussian98*, Revision A.11.1; Gaussian Inc.: Pittsburgh, PA, 2001.

(37) Pesce-Rodriguez, R. A. Thermal decomposition of HNIW based formulations 92, 9, ADA255613.

(38) Foltz, M. F. Thermal stability of the polymorphs of hexanitrohexaazaisowurtzitane, Part I, 94, EIP94071330965.

(39) Foltz, M. F. Thermal stability of the polymorphs of hexanitrohexaazaisowurtzitane, Part II, 94, EIP94091387087.

(40) Foltz, M. F. Thermal stability of episilon-hexanitrohexaazaisowurtzitane in an Estane formulation, Part I, 94, EIP94091384867.

(41) Harris, N. J.; Lammertsma, K. *J. Am. Chem. Soc.* **1997**, *119*, 6583.

(42) Qasim, M.; Fredrickson, H. L.; Furey, J.; Castellane, R.; McGrath, C.; Szecsody, J. *Abstracts of the 4th Southern School on Computational Chemistry*; Orange Beach, AL, 2004; p 90.